

# $\tau$ data-driven evaluation of Euclidean windows for the hadronic vacuum polarization

Pere Masjuan <sup>\*1,2</sup>, Alejandro Miranda <sup>†2</sup>, and Pablo Roig <sup>‡3</sup>

<sup>1</sup>Grup de Física Teòrica, Departament de Física, Universitat Autònoma de Barcelona, 08193 Bellaterra (Barcelona), Spain.

<sup>2</sup>Institut de Física d'Altes Energies (IFAE) and The Barcelona Institute of Science and Technology (BIST), Campus UAB, 08193 Bellaterra (Barcelona), Spain.

<sup>3</sup>Departamento de Física, Centro de Investigación y de Estudios Avanzados del Instituto Politécnico Nacional, Apdo. Postal 14-740, 07000 Ciudad de México, México

## Abstract

We compute for the first time the  $\tau$  data-driven Euclidean windows for the hadronic vacuum polarization contribution to the muon  $g-2$ . We show that  $\tau$ -based results agree with the available lattice window evaluations and with the full result. On the intermediate window, where all lattice evaluations are rather precise and agree,  $\tau$ -based results are compatible with them. This is particularly interesting, given that the disagreement of the  $e^+e^-$  data-driven result with the lattice values in this window is the main cause for their discrepancy, affecting the interpretation of the  $a_\mu$  measurement in terms of possible new physics.

## 1 Introduction

The first Fermilab measurement of the muon anomalous magnetic moment ( $a_\mu = (g_\mu - 2)/2$ , with  $g$  the gyromagnetic factor) confirmed [1] the final result from Brookhaven [2], yielding the world average

$$a_\mu^{\text{Exp}} \times 10^{11} = 116592061(41). \quad (1)$$

This reaffirmed and strengthened the interest of the high-energy physics community in this observable, given its  $4.2\sigma$  tension with the Standard Model prediction [3–37], obtained within the Muon  $g-2$  Theory Initiative [38] <sup>1</sup>

$$a_\mu^{\text{SM}} \times 10^{11} = 116591810(43). \quad (2)$$

However, the BMWc lattice Collaboration published [66] a precise lattice-QCD evaluation of the hadronic vacuum polarization (HVP) contribution with the result

$$a_\mu^{\text{BMWc}} \times 10^{10} = 707.5 \pm 5.5, \quad (3)$$

which yields an  $a_\mu$  evaluation at  $1.5\sigma$  from  $a_\mu^{\text{Exp}}$ , Eq. (1), and at  $2.1\sigma$  from the data-driven result, based on  $\sigma(e^+e^- \rightarrow \text{hadrons})$ , that was employed to get Eq. (2). A direct comparison between the BMWc and data-driven predictions for the HVP contribution can be found in Table 4.

---

<sup>\*</sup>masjuan@ifae.es

<sup>†</sup>jmiranda@ifae.es

<sup>‡</sup>pablo.roig@investav.mx

<sup>1</sup>See later developments in e.g. Refs. [39–65].

Recently, other three accurate lattice evaluations, by the Mainz CLS [67], the ETMC [68] and the RBC/UKQCD [62] collaborations, have agreed within the so-called intermediate window (defined below, in Eq. (6)) with the BMWc result, having commensurate uncertainties.

Reference [69], which sets the foundations to start this project, has translated the data-driven results to the three different windows in Euclidean time used by lattice practitioners, to scrutinize the root of the current discrepancy between both groups of results. This is a crucial endeavour, since it currently limits the implications on new physics of the  $a_\mu$  measurements, as may help to pinpoint in what energy domain discrepancies emerge<sup>2</sup>. It is also a timely task, as we expect the soon release of the second  $a_\mu$  FNAL value, with improved precision, in the forthcoming months<sup>3</sup>.

The situation has become even more puzzling with the recent accurate  $\sigma(e^+e^- \rightarrow \pi^+\pi^-)$ <sup>4</sup> CMD-3 measurement [76, 77], which would -on its own- reduce the discrepancy with  $a_\mu^{\text{Exp}}$  to less than two standard deviations. Consequently, it is in tension with the previous measurements of this reaction, by CMD-2 [78–81], SND [82, 83], KLOE [84–87], BaBar [88], BES [89] and CLEO [90]. Dedicated studies related to the radiative corrections employed in the Monte Carlo generators used by these experiments [91] (see e.g. Refs. [92–94]) could provide more insight into this matter.

Within the data-driven evaluations of  $a_\mu^{\text{HVP}}$ ,  $\tau^- \rightarrow \nu_\tau$  hadrons was proposed in 1997 to reduce the error (by  $\sim 37\%$  then) of the method when using only  $e^+e^- \rightarrow \text{hadrons}$  in LEP times [95]. Through the years, this alternative data-driven method has always been [96–101] approximately  $[2, 2.5]\sigma$  away from the  $a_\mu^{\text{Exp}}$  world average, a situation which seems now favored by the lattice QCD evaluations of  $a_\mu^{\text{HVP}}$ <sup>5</sup>. Still, a direct comparison between lattice QCD results and  $\tau$  data-driven methodology is not straightforward either. This motivates us to compute in this work Euclidean windows for  $a_\mu^{\text{HVP}}$  using  $\tau$  data and compare results. We hope our outcomes may shed some light on this puzzling situation<sup>6</sup> and be useful for the lattice effort [106] to compute the required isospin-breaking corrections (see below Eq. (6)) entering the  $\tau$ -based method. In section 2 we explain the needed formulae and apply them to obtain the results, which are summarized in section 3.

## 2 Results

The HVP contribution at leading order (LO) in the data-driven approach is given by [107–110]

$$a_\mu^{\text{HVP,LO}} = \frac{1}{4\pi^3} \int_{s_{\text{thr}}}^\infty ds K(s) \sigma_{e^+e^- \rightarrow \text{hadrons}(+\gamma)}^0(s), \quad (4)$$

where  $\sigma_{e^+e^- \rightarrow \text{hadrons}(+\gamma)}^0(s)$  is the bare hadronic cross-section, which excludes effects from vacuum polarization (VP) [111], and  $K(s)$  is a smooth kernel concentrated at low energies [109, 112]

$$K(s) = \frac{x^2}{2}(2 - x^2) + \frac{(1 + x^2)(1 + x)^2}{x^2} \left( \log(1 + x) - x + \frac{x^2}{2} \right) + \frac{(1 + x)}{(1 - x)} x^2 \log(x), \quad (5)$$

which is written in terms of the variable  $x = \frac{1 - \beta_\mu}{1 + \beta_\mu}$ ,  $\beta_\mu = \sqrt{1 - 4m_\mu^2/s}$ . This dispersive approach revolves around the handiness of  $e^+e^-$  hadronic cross-section measurements at energies below a few GeV. However, as was pointed out early by Alemany, Davier, and Höcker [95], it is also possible to use hadronic  $\tau$  decays to evaluate the HVP, LO contributions to  $a_\mu$ . For some time this approach

<sup>2</sup>Additionally, a data-driven estimation for the isospin-limit light-quark connected component of the intermediate-window contribution ( $a_\mu^{\text{win,lqc}}$ ) [70] is in significant tension with recent very-precise lattice-QCD predictions [62, 66–68, 71–74], showing that the difference between data-driven and lattice-QCD outcomes for  $a_\mu^{\text{win}}$  is almost completely ascribed to the light-quark connected contribution.

<sup>3</sup>Indeed it was during the refereeing of this article, [75].

<sup>4</sup>This contribution yields a bit more than 70% of  $a_\mu^{\text{HVP,LO}}$ .

<sup>5</sup>The difference between both data-driven groups of results could also be due to non-standard interactions modifying slightly -but noticeably at this precision- the di-pion  $\tau$  decays [102–105].

<sup>6</sup>We acknowledge that if good agreement was found amid  $e^+e^- \rightarrow \pi^+\pi^-$  measurements, di-pion tau decays could not possibly contribute, since the error associated to the required isospin-breaking corrections would be larger than the uncertainties of the cross-section measurements.

was competitive with the  $e^+e^-$  data, although this is generally not considered the case at the moment [38].

Recently, a new  $\tau$  data-driven approach was performed in Ref. [101]. In this section, we utilize their results to evaluate the leading HVP contribution to the anomalous magnetic moment of the muon in the so-called window quantities [12, 71]. For this enterprise, we make use of the weight functions in center-of-mass energy  $\tilde{\Theta}(s)$  from Eq. (12) in Ref. [69] which are related to those in Euclidean time [12]

$$\begin{aligned}\Theta_{SD}(t) &= 1 - \Theta(t, t_0, \Delta), \\ \Theta_{win}(t) &= \Theta(t, t_0, \Delta) - \Theta(t, t_1, \Delta), \\ \Theta_{LD}(t) &= \Theta(t, t_1, \Delta), \\ \Theta(t, t', \Delta) &= \frac{1}{2} \left( 1 + \tanh \frac{t - t'}{\Delta} \right).\end{aligned}\tag{6}$$

The subscripts in Eq. (6) refer to the short-distance ( $SD$ ), intermediate ( $win$ , although we will use  $int$  in the following) and long-distance ( $LD$ ) contributions with parameters

$$t_0 = 0.4 \text{ fm}, \quad t_1 = 1.0 \text{ fm}, \quad \Delta = 0.15 \text{ fm},\tag{7}$$

which correspond to inverse energies of the order of 500, 200 and 1300 MeV, respectively.

In what follows, we will focus on the dominant  $2\pi$  contribution only. Including isospin breaking (IB) corrections, i.e.,  $\mathcal{O}[(m_u - m_d)p^2]$  and  $\mathcal{O}(e^2 p^2)$  contributions, the *bare* hadronic  $e^+e^-$  cross-section  $\sigma_{\pi\pi(\gamma)}^0$  is related to the *observed* differential  $\tau$  decay rate  $d\Gamma_{\pi\pi[\gamma]}$  through [96, 97]

$$\sigma_{\pi\pi(\gamma)}^0 = \left[ \frac{K_\sigma(s)}{K_\Gamma(s)} \frac{d\Gamma_{\pi\pi[\gamma]}}{ds} \right] \times \frac{R_{IB}(s)}{S_{EW}},\tag{8}$$

where

$$\begin{aligned}K_\Gamma(s) &= \frac{G_F^2 |V_{ud}|^2 m_\tau^3}{384\pi^3} \left( 1 - \frac{s}{m_\tau^2} \right)^2 \left( 1 + \frac{2s}{m_\tau^2} \right), \\ K_\sigma(s) &= \frac{\pi\alpha^2}{3s},\end{aligned}\tag{9}$$

and the IB corrections are encoded in

$$R_{IB}(s) = \frac{\text{FSR}(s)}{G_{EM}(s)} \frac{\beta_{\pi^+\pi^-}^3}{\beta_{\pi^+\pi^0}^3} \left| \frac{F_V(s)}{f_+(s)} \right|^2.\tag{10}$$

The  $S_{EW}$  term in Eq. (8) includes the short-distance electroweak corrections [113–120]. FSR refers to the Final-State-Radiation corrections to the  $\pi^+\pi^-$  channel [121, 122]<sup>7</sup>, while the  $G_{EM}(s)$  factor includes the QED corrections to the  $\tau^- \rightarrow \pi^-\pi^0\nu_\tau$  decay with virtual plus real photon radiation.  $\beta_{\pi^-\pi^+}^3/\beta_{\pi^-\pi^0}^3$  is a phase space correction owing to the  $\pi^\pm - \pi^0$  mass difference. The last term in  $R_{IB}(s)$  corresponds to the ratio between the neutral ( $F_V(s)$ ) and the charged ( $f_+(s)$ ) pion form factor, which includes one of the leading IB effects, the  $\rho^0 - \omega$  mixing correction.

The IB corrections to  $a_\mu^{\text{HVP, LO}}$  using  $\tau$  data in the dominant  $\pi\pi$  channel [123, 124] can be evaluated using the following expression [98]

$$\Delta a_\mu^{\text{HVP, LO}}[\pi\pi, \tau] = \frac{1}{4\pi^3} \int_{4m_\pi^2}^{m_\tau^2} ds K(s) \left[ \frac{K_\sigma(s)}{K_\Gamma(s)} \frac{d\Gamma_{\pi\pi[\gamma]}}{ds} \right] \left( \frac{R_{IB}(s)}{S_{EW}} - 1 \right),\tag{11}$$

which measures the difference between the correct expression for  $\sigma_{\pi\pi(\gamma)}^0$  and the naive Conserved Vector Current approximation, with  $S_{EW} = 1$  and  $R_{IB}(s) = 1$ .

These contributions are summarized in Table 1 for each IB correction.

---

<sup>7</sup>To our knowledge, FSR was not included in  $R_{IB}$  before Ref. [98].

- The  $S_{\text{EW}}$  factor ( $S_{\text{EW}} = 1.0233(3)$ , at the scale  $m_\tau$ ) contributes 3.0%, 28.7% and 68.3% to the complete  $\Delta a_\mu^{\text{HVP, LO}} = -11.96(0) \cdot 10^{-10}$  correction for the  $SD$ ,  $\text{int}$  and  $LD$  contributions, respectively <sup>8</sup>.
- The phase space (PS) correction yields 1.7%, 18.7% and 79.6% of a total of  $\Delta a_\mu^{\text{HVP, LO}} = -7.47(0) \cdot 10^{-10}$  for the  $SD$ ,  $\text{int}$  and  $LD$  contributions, respectively.
- The final state radiation (FSR) induces 2.9%, 27.0% and 70.1% of a total of  $\Delta a_\mu^{\text{HVP, LO}} = +4.56(45) \cdot 10^{-10}$  for the  $SD$ ,  $\text{int}$  and  $LD$  contributions, respectively.
- $G_{\text{EM}}(s)$  was originally computed in Ref. [97] including those operators yielding resonance saturation of the  $\mathcal{O}(p^4)$  chiral couplings in the frame of Resonance Chiral Theory (R $\chi$ T) [127–130] <sup>9 10</sup>, which comprises Goldstone bosons and resonance fields extending the  $\chi$ PT framework [134–136] to higher energies. A recalculation of  $G_{\text{EM}}(s)$  was performed later in [137, 138] using a Vector Meson Dominance (VMD) model [139].  
In Ref. [101] (see also [140]), two of us explored the impact of the R $\chi$ T operators contributing to resonance saturation at the next chiral order ( $\mathcal{O}(p^6)$ ) on the  $G_{\text{EM}}(s)$ , as well as estimating the uncertainty of the original computation in [97]. These results [101] are consistent with the earlier R $\chi$ T and the VMD estimates [101]. Availing of these results,  $G_{\text{EM}}(s)$  produces a correction of  $\sim -3.5\%$ ,  $\sim -17.1\%$  and  $\sim +120.6\%$  of  $\Delta a_\mu^{\text{HVP, LO}} = -1.71_{(1.48)}^{(0.61)} \cdot 10^{-10}$  at  $\mathcal{O}(p^4)$ , and  $\sim 0.4\%$ ,  $\sim 7.6\%$  and  $\sim 92.0\%$  of  $\Delta a_\mu^{\text{HVP, LO}} = -7.59_{(4.56)}^{(6.50)} \cdot 10^{-10}$  at  $\mathcal{O}(p^6)$  for the  $SD$ ,  $\text{int}$  and  $LD$  contributions, respectively. Interestingly, the  $SD$  and  $\text{int}$  contributions at  $\mathcal{O}(p^4)$  change in sign while this is not the case at  $\mathcal{O}(p^6)$  where all the contributions are always negative.
- The ratio of the form factors (FF) gives an overall correction of  $\Delta a_\mu^{\text{HVP, LO}} = +7.13(1.48)_{(1.54)}^{(1.59)}_{(0.80)} \cdot 10^{-10}$ , from which  $\sim 2.2\%$ ,  $\sim 26.8\%$  and  $\sim 71.0\%$  stand for the  $SD$ ,  $\text{int}$  and  $LD$  corrections, respectively.

The errors quoted in this contribution correspond to the electromagnetic shifts in the widths and masses of the  $\rho$  meson, and to the  $\rho^0 - \omega$  mixing parameter [97, 141] (see Eqs. (5.5) and (5.6) in Ref. [97]), respectively <sup>11</sup>. For this analysis, we use the same numerical inputs as in [101]. The central value reported in Table 1 corresponds to the weighted average between the FF1 and FF2 sets <sup>12</sup>.

The overall correction is also consistent with those in Refs. [97, 98, 101].

$\Delta a_\mu^{\text{HVP, LO}}$							
	SD		int		LD		Total
	$\mathcal{O}(p^4)$	$\mathcal{O}(p^6)$	$\mathcal{O}(p^4)$	$\mathcal{O}(p^6)$	$\mathcal{O}(p^4)$	$\mathcal{O}(p^6)$	$\mathcal{O}(p^4)$ $\mathcal{O}(p^6)$
$S_{\text{EW}}$	-0.36(0)		-3.43(0)		-8.17(0)		-11.96(0)
PS	-0.13(0)		-1.39(0)		-5.95(0)		-7.47(0)
FSR	+0.13(1)		+1.23(12)		+3.20(32)		+4.56(46)
$G_{\text{EM}}$	+0.06 <sub>(2)</sub> <sup>(9)</sup>	-0.03 <sub>(7)</sub> <sup>(9)</sup>	+0.29 <sub>(19)</sub> <sup>(6)</sup>	-0.58 <sub>(71)</sub> <sup>(93)</sup>	-2.06 <sub>(1.27)</sub> <sup>(0.55)</sup>	-7.00 <sub>(3.78)</sub> <sup>(5.48)</sup>	-1.71 <sub>(1.48)</sub> <sup>(0.61)</sup> -7.61 <sub>(4.56)</sub> <sup>(6.50)</sup>
FF	+0.16(5)(1) <sub>(7)</sub> <sup>(1)</sup>		+1.91(49) <sub>(27)</sub> <sup>(29)</sup>	-2.26 <sub>(20)</sub> <sup>(12)</sup>	+5.06(94) <sub>(1.26)</sub> <sup>(1.29)</sup>	+7.13(1.48) <sub>(1.54)</sub> <sup>(1.59)</sup>	+7.13(1.48) <sub>(1.54)</sub> <sup>(1.59)</sup>
Total	-0.14(6)	-0.23 <sub>(9)</sub> <sup>(11)</sup>	-1.39 <sub>(64)</sub> <sup>(62)</sup>	-2.26 <sub>(0.93)</sub> <sup>(1.12)</sup>	-7.92 <sub>(2.13)</sub> <sup>(1.83)</sup>	-12.86 <sub>(4.15)</sub> <sup>(5.75)</sup>	-9.45 <sub>(2.83)</sub> <sup>(2.51)</sup> -15.35 <sub>(5.17)</sub> <sup>(6.98)</sup>

Table 1:  $\Delta a_\mu^{\text{HVP, LO}}$  in units of  $10^{-10}$ . The uncertainties in the fifth row (FF) are related to  $\Delta\Gamma_\rho$ ,  $\Delta M_\rho$  and  $\theta_{\omega\rho}$ , respectively.

<sup>8</sup>We are correcting here our double-counting [101] of the subleading non-logarithmic short-distance correction for quarks, as noted in ref. [125] (see ref. [126]).

<sup>9</sup>We will shorten this to ‘ $\mathcal{O}(p^4)$ ’ for brevity, and similarly at the next chiral order. In the first case, short-distance QCD behaviour is ensured for two point Green functions, while this is extended up to 3-point correlators in the latter.

<sup>10</sup>Pseudoscalar pole (axial) contributions to the hadronic light-by-light piece of  $a_\mu$  have been computed within R $\chi$ T [131, 132] ([31]), as well as di-meson contributions to  $a_\mu^{\text{HVP}}$  [65, 133].

<sup>11</sup>We note that, according to refs. [5, 57, 142], this correction is smaller in data-driven methods than in phenomenological estimates. The associated uncertainties, however, are subleading in our analysis, as we have checked in detail, accounting for these errors, in the comparisons shown in fig. 3.

<sup>12</sup>The main distinction between FF1 and FF2 comes from the width difference between the  $\rho^\pm$  and  $\rho^0$  mesons ( $\Delta\Gamma_\rho = \Gamma_{\rho^0} - \Gamma_{\rho^\pm}$ ), while the mass difference ( $\Delta M_\rho = M_{\rho^0} - M_{\rho^\pm}$ ) and the  $\theta_{\omega\rho}$  parameter are the same in both.

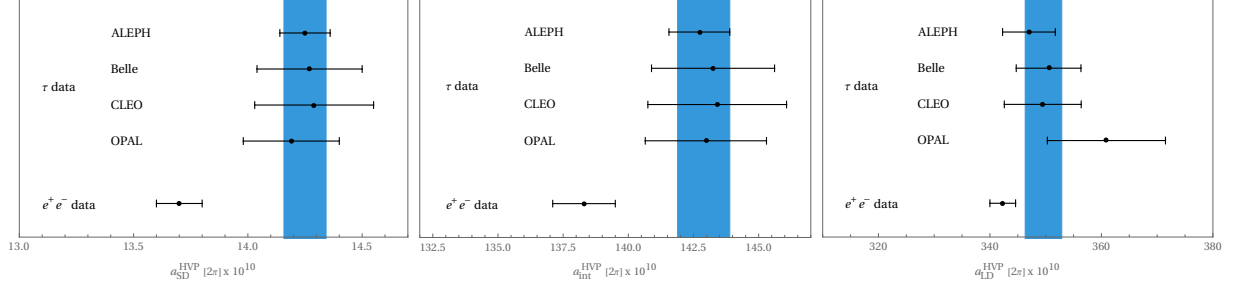


Figure 1: Windows quantities for HVP at  $\mathcal{O}(p^4)$  for  $2\pi$  below 1.0 GeV using the parameters in Eq. (7). The blue region corresponds to the experimental average from  $\tau$  data. The  $e^+e^-$  number was taken from Ref. [69].

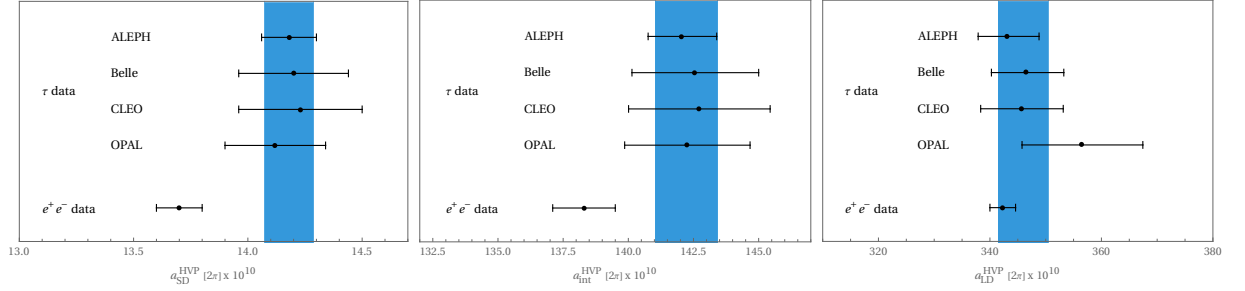


Figure 2: Analog to Fig. 1 but at  $\mathcal{O}(p^6)$ .

Using the  $\tau$  spectral functions measured by ALEPH [143], Belle [144], CLEO [145] and OPAL [146], we evaluate  $a_\mu^{\text{HVP, LO}}[\pi\pi]$  using the window parameters in Eq. (7). These results are outlined in Tables 2 and 3 for  $s \leq 1, 2, 3$ , and  $3.125 \text{ GeV}^2$ , i.e., integrating Eq. (4) with  $\sigma_{\pi\pi(\gamma)}^0$  in Eq. (8) from  $s_{\text{thr}} = 4m_\pi^2$  up to some given cut-off. In the aforementioned tables 2 and 3, the first uncertainty is connected to the systematic errors on the mass spectrum, and from the  $\tau$ -mass and  $V_{ud}$  uncertainties; the second error is associated to  $B_{\pi\pi^0}$  and  $B_e$ ; and the third one is due to the IB corrections. The *Mean* value in the tables corresponds to the weighted average from the different window contributions for each experiment, the first error is related to the experimental measurements, while the second one comes from the IB corrections.

An evaluation of  $a_\mu^{\text{HVP}}$  in the windows in Euclidean time using  $e^+e^-$  data was performed in Ref. [69] using the parameters in Eq. (7), see Table 4 below. A comparison between these window quantities for HVP in the  $2\pi$  channel below 1 GeV amounts to a discrepancy of  $4.3\sigma$ ,  $3.2\sigma$  and  $2.1\sigma$  between the  $\tau$  and  $e^+e^-$  evaluations applying the  $G_{\text{EM}}(s)$  correction at  $\mathcal{O}(p^4)$  in  $R_X T$  to the  $\tau$  data for the  $SD$ ,  $int$  and  $LD$  contributions, respectively. On the other hand, when we include the corrections at  $\mathcal{O}(p^6)$ , the difference between these two evaluations decreases to  $3.6\sigma$ ,  $2.6\sigma$  and  $0.9\sigma$  for the  $SD$ ,  $int$  and  $LD$  contributions, respectively. These results are depicted in Figs. 1 and 2, where the blue band corresponds to the experimental average using  $\tau$  data. Fig. 3 shows a zoomed comparison between  $\tau$  (after IB corrections at  $\mathcal{O}(p^6)$ ) and  $e^+e^- \rightarrow \pi^+\pi^-$  spectral function using the ISR measurements from BABAR [88] and KLOE [86] (left-hand panel) and the energy-scan measurements from CMD-3 [76] (right-hand panel). Colored bands correspond to the weighted average of the uncertainties coming from both sets of data in each figure. Although it may seem obvious that increased IB-corrections in the  $\rho$  region will increase the compatibility between  $\tau$  and CMD-3  $e^+e^-$  data, dedicated studies (like e.g. Ref. [147]) seem necessary to fully understand this issue (even more in the comparison with KLOE and BaBar).

A direct comparison between  $a_\mu^{\text{HVP, LO}}[\pi\pi, \tau]$  and the lattice results is not possible. For that endeavour, it is necessary to supplement the  $2\pi$  evaluation with the remaining contributions from all other channels accounting for the hadronic cross-section. To illustrate the impact of this con-

$a_\mu^{\text{HVP,LO}}[\pi\pi, \tau]$				
SD				
Experiment	$s \leq 1 \text{ GeV}^2$	$s \leq 2 \text{ GeV}^2$	$s \leq 3 \text{ GeV}^2$	$s \leq 3.125 \text{ GeV}^2$
ALEPH	14.25(4)(8)(6)	15.46(2)(9)(6)	15.52(3)(9)(6)	15.52(3)(9)(6)
Belle	14.27(4)(22)(6)	15.34(5)(24)(6)	15.39(6)(24)(6)	15.41(12)(24)(6)
CLEO	14.29(6)(25)(6)	15.41(6)(27)(6)	15.45(6)(27)(6)	15.46(6)(27)(6)
OPAL	14.19(7)(19)(6)	15.46(3)(21)(6)	15.51(3)(21)(6)	15.51(3)(21)(6)
Mean	14.25(7)(6)	15.44(8)(6)	15.50(8)(6)	15.50(8)(6)
Intermediate				
Experiment	$s \leq 1 \text{ GeV}^2$	$s \leq 2 \text{ GeV}^2$	$s \leq 3 \text{ GeV}^2$	$s \leq 3.125 \text{ GeV}^2$
ALEPH	142.73(61)(79) $^{(61)}_{(63)}$	149.02(50)(83) $^{(61)}_{(63)}$	149.18(48)(83) $^{(61)}_{(63)}$	149.18(48)(83) $^{(61)}_{(63)}$
Belle	143.25(45)(2.24) $^{(61)}_{(63)}$	148.83(48)(2.33) $^{(62)}_{(64)}$	148.97(49)(2.33) $^{(62)}_{(64)}$	149.00(54)(2.33) $^{(62)}_{(64)}$
CLEO	143.41(60)(2.52) $^{(61)}_{(63)}$	149.23(61)(2.62) $^{(62)}_{(64)}$	149.34(61)(2.62) $^{(62)}_{(64)}$	149.37(61)(2.62) $^{(62)}_{(64)}$
OPAL	142.98(1.17)(1.92) $^{(60)}_{(62)}$	149.56(97)(2.01) $^{(60)}_{(63)}$	149.69(97)(2.01) $^{(60)}_{(63)}$	149.69(97)(2.01) $^{(60)}_{(63)}$
Mean	142.89(81) $^{(61)}_{(63)}$	149.09(80) $^{(61)}_{(64)}$	149.23(79) $^{(61)}_{(64)}$	149.24(79) $^{(61)}_{(64)}$
LD				
Experiment	$s \leq 1 \text{ GeV}^2$	$s \leq 2 \text{ GeV}^2$	$s \leq 3 \text{ GeV}^2$	$s \leq 3.125 \text{ GeV}^2$
ALEPH	347.03(4.12)(1.93) $^{(1.27)}_{(1.47)}$	350.79(4.08)(1.95) $^{(1.27)}_{(1.47)}$	350.83(4.08)(1.95) $^{(1.27)}_{(1.47)}$	350.83(4.08)(1.95) $^{(1.27)}_{(1.47)}$
Belle	350.55(1.36)(5.49) $^{(1.27)}_{(1.48)}$	353.90(1.37)(5.54) $^{(1.28)}_{(1.49)}$	353.93(1.37)(5.55) $^{(1.28)}_{(1.49)}$	353.93(1.37)(5.55) $^{(1.27)}_{(1.48)}$
CLEO	349.49(2.88)(6.13) $^{(1.27)}_{(1.47)}$	353.00(2.88)(6.20) $^{(1.27)}_{(1.47)}$	353.02(2.88)(6.20) $^{(1.27)}_{(1.48)}$	353.03(2.88)(6.20) $^{(1.27)}_{(1.47)}$
OPAL	360.91(9.33)(4.85) $^{(1.26)}_{(1.51)}$	364.82(9.26)(4.90) $^{(1.25)}_{(1.51)}$	364.84(9.26)(4.90) $^{(1.26)}_{(1.51)}$	364.84(9.26)(4.90) $^{(1.26)}_{(1.51)}$
Mean	349.65(3.01) $^{(1.27)}_{(1.48)}$	353.25(3.01) $^{(1.27)}_{(1.48)}$	353.28(3.01) $^{(1.27)}_{(1.49)}$	353.28(3.01) $^{(1.27)}_{(1.48)}$

Table 2: IB-corrected  $a_\mu^{\text{HVP,LO}}[\pi\pi, \tau]$  in units of  $10^{-10}$  at  $\mathcal{O}(p^4)$  in  $\text{R}\chi\text{T}$  using the experimental measurements from the ALEPH [143], Belle [144], CLEO [145] and OPAL [146] Colls. The first error is related to the systematic uncertainties on the mass spectrum and also includes contributions from the  $\tau$ -mass and  $V_{ud}$  uncertainties. The second error arises from  $B_{\pi\pi^0}$  and  $B_e$ , and the third error comes from the isospin-breaking corrections. The uncertainties in the mean value correspond to the experiment and to the IB corrections, respectively.

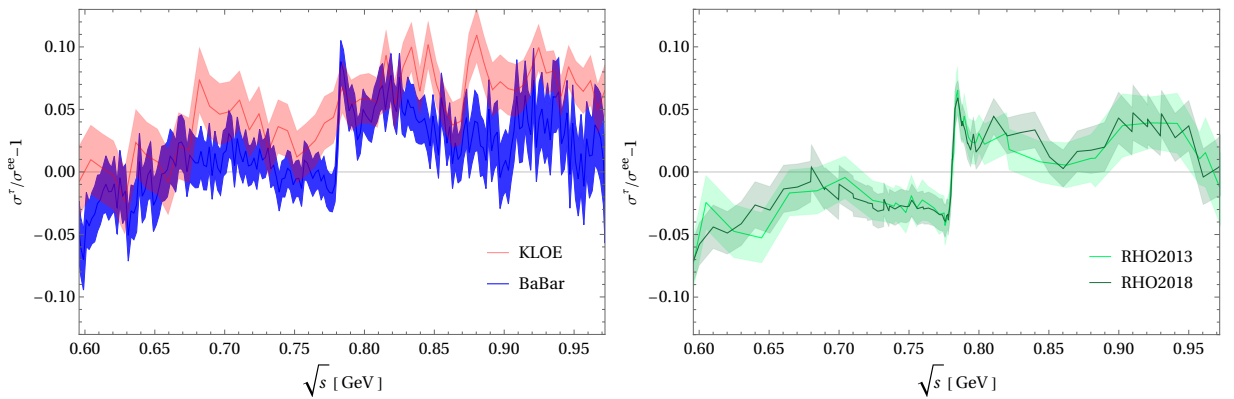


Figure 3: Comparison between the  $\tau$  (after IB corrections) and  $e^+e^- \rightarrow \pi^+\pi^-$  spectral function using the ISR measurements from BABAR [88] and KLOE [86] (left-hand) and the energy-scan measurements from CMD-3 [76] (right-hand).

$a_\mu^{\text{HVP,LO}}[\pi\pi, \tau]$				
SD				
Experiment	$s \leq 1 \text{ GeV}^2$	$s \leq 2 \text{ GeV}$	$s \leq 3 \text{ GeV}$	$s \leq 3.125 \text{ GeV}^2$
ALEPH	14.18(4)(8)(8)	15.37(2)(9)( $^{11}_9$ )	15.42(2)(9)( $^{11}_9$ )	15.42(3)(9)( $^{11}_9$ )
Belle	14.20(4)(22)(8)	15.25(5)(24)( $^{10}_8$ )	15.30(5)(24)( $^{10}_8$ )	15.31(12)(24)( $^{10}_8$ )
CLEO	14.23(6)(25)(8)	15.32(6)(27)( $^{10}_8$ )	15.36(6)(27)( $^{10}_9$ )	15.37(6)(27)( $^{10}_9$ )
OPAL	14.12(7)(19)(8)	15.37(3)(21)( $^{11}_9$ )	15.41(3)(21)( $^{11}_9$ )	15.41(3)(21)( $^{11}_9$ )
Mean	14.18(7)(8)	15.35(8)( $^{11}_9$ )	15.40(8)( $^{11}_9$ )	15.41(8)( $^{11}_9$ )
Intermediate				
Experiment	$s \leq 1 \text{ GeV}^2$	$s \leq 2 \text{ GeV}^2$	$s \leq 3 \text{ GeV}^2$	$s \leq 3.125 \text{ GeV}^2$
ALEPH	142.04(60)(79)( $^{94}_{83}$ )	148.21(50)(83)( $^{1.04}_{89}$ )	148.35(48)(83)( $^{1.04}_{89}$ )	148.35(48)(83)( $^{1.04}_{89}$ )
Belle	142.55(45)(2.23)( $^{94}_{83}$ )	148.03(48)(2.32)( $^{1.04}_{90}$ )	148.16(48)(2.32)( $^{1.05}_{90}$ )	148.19(54)(2.32)( $^{1.05}_{90}$ )
CLEO	142.71(60)(2.50)( $^{94}_{83}$ )	148.41(60)(2.60)( $^{1.03}_{89}$ )	148.52(60)(2.61)( $^{1.03}_{89}$ )	148.55(60)(2.61)( $^{1.03}_{89}$ )
OPAL	142.24(1.16)(1.91)( $^{98}_{85}$ )	148.68(95)(2.00)( $^{1.08}_{92}$ )	148.80(95)(2.00)( $^{1.09}_{92}$ )	148.80(95)(2.00)( $^{1.09}_{92}$ )
Mean	142.19(80)( $^{95}_{84}$ )	148.26(79)( $^{1.05}_{90}$ )	148.40(79)( $^{1.05}_{90}$ )	148.41(79)( $^{1.05}_{90}$ )
LD				
Experiment	$s \leq 1 \text{ GeV}^2$	$s \leq 2 \text{ GeV}^2$	$s \leq 3 \text{ GeV}^2$	$s \leq 3.125 \text{ GeV}^2$
ALEPH	343.09(3.99)(1.91)( $^{3.65}_{2.78}$ )	346.78(3.95)(1.93)( $^{3.71}_{2.83}$ )	346.81(3.95)(1.93)( $^{3.71}_{2.83}$ )	346.81(3.95)(1.93)( $^{3.71}_{2.83}$ )
Belle	346.53(1.34)(5.43)( $^{3.75}_{2.86}$ )	349.82(1.35)(5.48)( $^{3.80}_{2.90}$ )	349.84(1.35)(5.48)( $^{3.80}_{2.90}$ )	349.84(1.36)(5.48)( $^{3.80}_{2.90}$ )
CLEO	345.55(2.77)(6.06)( $^{3.67}_{2.80}$ )	348.99(2.77)(6.12)( $^{3.72}_{2.85}$ )	349.01(2.77)(6.12)( $^{3.72}_{2.85}$ )	349.02(2.77)(6.13)( $^{3.72}_{2.85}$ )
OPAL	356.42(8.99)(4.79)( $^{4.21}_{3.18}$ )	360.25(8.92)(4.84)( $^{4.27}_{3.22}$ )	360.28(8.92)(4.84)( $^{4.27}_{3.22}$ )	360.28(8.92)(4.84)( $^{4.27}_{3.22}$ )
Mean	345.65(2.95)( $^{3.82}_{2.91}$ )	349.17(2.95)( $^{3.88}_{2.95}$ )	349.19(2.95)( $^{3.88}_{2.95}$ )	349.20(2.95)( $^{3.88}_{2.95}$ )

Table 3: Same as Table 2, but the  $\mathcal{O}(p^6)$  contributions to  $G_{\text{EM}}(s)$  in Ref. [101] have been applied to the  $\tau$  data.

tribution in  $a_\mu^{\text{HVP, LO}}$ , we follow two approaches<sup>13</sup>. Firstly, using the values reported in Table 1 of Ref. [69] we subtract the contribution from the  $2\pi$  channel below 1.0 GeV (we represent this procedure with ' $< 1 \text{ GeV}$ ') and replace it by the corresponding mean value in Tables 2 and 3. This way, we get

$$a_\mu^{SD} = 69.0(5) \times 10^{-10}, \quad a_\mu^{int} = 234.0(1.2) \times 10^{-10}, \quad a_\mu^{LD} = 402.5(3.3) \times 10^{-10}, \quad (12)$$

at  $\mathcal{O}(p^4)$ , and

$$a_\mu^{SD} = 68.9(5) \times 10^{-10}, \quad a_\mu^{int} = 233.3(1.4) \times 10^{-10}, \quad a_\mu^{LD} = 398.5(4.9) \times 10^{-10}, \quad (13)$$

at  $\mathcal{O}(p^6)$ .

Secondly, we estimate the  $2\pi$  full contribution using the ratios  $a_\mu^I/a_\mu^{\text{HVP, LO}}$ , where  $I$  stands for  $SD$ ,  $int$  and  $LD$ , from the corresponding window quantities in Ref. [69] and the overall weighted-average evaluation of  $a_\mu^{\text{HVP, LO}}[\pi\pi, e^+e^-] = 505.1(1.7) \times 10^{-10}$  in Refs. [7, 8]. However, as can be easily computed from Tables 2 and 3, these ratios are not the same between the second and the last column. This effect is mainly due to the weight functions  $\hat{\Theta}(s)$  in Eq. (6)<sup>14</sup>, so, in order to take this into account, we use the difference between the ratio from the second and third column to correct the ratios from  $e^+e^-$  data. Then we subtract this value from the total contribution and replace it by our results<sup>15</sup>. Finally, we get

$$a_\mu^{SD} = 69.0(7) \times 10^{-10}, \quad a_\mu^{int} = 234.2(2.0) \times 10^{-10}, \quad a_\mu^{LD} = 402.6(3.8) \times 10^{-10}, \quad (14)$$

<sup>13</sup>In this exploratory study correlations between different energy ranges in the two pion channel and also between the two pion and other channels are neglected. We plan to improve this within the joint effort of the muon  $g - 2$  theory initiative, <https://muon-gm2-theory.illinois.edu/>.

<sup>14</sup>We gratefully thank Michel Davier, Bogdan Malaescu and Zhiqing Zhang for pointing out an inconsistency in our earlier procedure, that we have now amended.

<sup>15</sup>Additionally, we have included a 50% uncertainty due to the difference between the ratios in the second and the last column to the final result.

at  $\mathcal{O}(p^4)$ , and

$$a_\mu^{SD} = 68.9(7) \times 10^{-10}, \quad a_\mu^{int} = 233.4(2.1) \times 10^{-10}, \quad a_\mu^{LD} = 398.5^{(5.3)}_{(4.6)} \times 10^{-10}, \quad (15)$$

at  $\mathcal{O}(p^6)$ . All these results are reasonably consistent with each other.

We summarize these outcomes in Table 4 along with the lattice results [12, 62, 66–68, 148] and other  $e^+e^-$  data-driven evaluations [38, 69]. These numbers are depicted in Fig. 4 for the intermediate window, where the blue band represents the weighted average of the lattice results,  $a_\mu^{int} = 235.8(6) \cdot 10^{-10}$ , excluding those from RBC/UKQCD 2018 [12] and ETMC 2021 [148] collaborations. The contributions of the intermediate window using  $\tau$  data are slightly closer to the results from lattice QCD than to the  $e^+e^-$  values. Therefore, the  $\sim 4.3\sigma$  discrepancy between the  $e^+e^-$  data-driven and lattice evaluations is reduced to  $\sim 1.5\sigma$  when  $\tau$  data is used for the  $2\pi$  channel. On the other hand, there is only one lattice result for the short-distance window [68] which seems to be in agreement with both data-driven HVP evaluations.

$a_\mu^{\text{HVP,LO}}$				
	SD	int	LD	Total
$\tau$ -data $\mathcal{O}(p^4) \leq 1 \text{ GeV}$	69.0(5)	234.0 <sup>(1.2)</sup> <sub>(1.3)</sub>	402.5 <sup>(3.3)</sup> <sub>(3.4)</sub>	705.5 <sup>(5.0)</sup> <sub>(5.2)</sub>
$\tau$ -data $\mathcal{O}(p^6) \leq 1 \text{ GeV}$	68.9(5)	233.3(1.4)	398.5 <sup>(4.9)</sup> <sub>(4.2)</sub>	700.7 <sup>(6.8)</sup> <sub>(6.1)</sub>
$\tau$ -data $\mathcal{O}(p^4)$	69.0(7)	234.2(2.0)	402.6 <sup>(3.8)</sup> <sub>(3.9)</sub>	705.8 <sup>(6.3)</sup> <sub>(6.6)</sub>
$\tau$ -data $\mathcal{O}(p^6)$	68.9(7)	233.4(2.1)	398.5 <sup>(5.3)</sup> <sub>(4.6)</sub>	700.8 <sup>(8.1)</sup> <sub>(7.4)</sub>
RBC/UKQCD 2018 [12]	—	231.9(1.5)	—	715.4(18.7)
ETMC 2021 [148]	—	231.7(2.8)	—	—
BMW 2020 [66]	—	236.7(1.4)	—	707.5(5.5)
Mainz/CLS 2022 [67]	—	237.30(1.46)	—	—
ETMC 2022 [68]	69.33(29)	235.0(1.1)	—	—
RBC/UKQCD 2023 [62]	—	235.56(82)	—	—
WP [38]	—	—	—	693.1(4.0)
BMW 2020/KNT [4, 66]	—	229.7(1.3)	—	—
Colangelo et al. 2022 [69]	68.4(5)	229.4(1.4)	395.1(2.4)	693.0(3.9)
Davier et al. 2023 [ $e^+e^-$ ] [147]	—	229.2(1.4)	—	694.0(4.0)
Davier et al. 2023 [ $\tau$ ] [125]	—	232.4(1.3)	—	—

Table 4: Window quantities for  $a_\mu^{\text{HVP,LO}}$  in units of  $10^{-10}$ . The first two rows correspond to the  $\tau$  evaluation in the first approach, while rows 3 and 4 are the evaluations in the second one. The rows 5–10 are the lattice results [12, 62, 66–68, 148]. The last three rows are the evaluations obtained using  $e^+e^-$  data. See Fig. 11 in Ref. [62] for more details.

### 3 Conclusions

While the BNL and FNAL measurements of  $a_\mu$  agree nicely within errors, the situation is not that clear for its SM prediction’s counterpart. On the one hand, data-driven methods based on  $e^+e^- \rightarrow \text{hadrons}$  data have to deal with the tensions between experiments (particularly among BaBar and KLOE, and now with CMD-3), which makes the computation of the uncertainty in Eq. (2) a non-trivial task, as will be its update. On the other side, there is still only one lattice QCD evaluation (BMWc Coll.) of  $a_\mu^{\text{HVP}}$  with competitive uncertainties, that lies between  $a_\mu^{\text{Exp}}$  and its SM data-driven prediction. However, the most recent Mainz/CLS, ETMC, and RBC/UKQCD results have similar errors to BMWc in the intermediate window, where all of them agree remarkably. It is long-known that alternative data-driven evaluations are possible, utilizing this time semileptonic  $\tau$ -decay data (and isospin-breaking corrections, with attached model-dependent uncertainty), as we have done here.

In this context, we have applied the study from Ref. [62], that computed window quantities in Euclidean time for data-driven evaluations of  $a_\mu^{\text{HVP}}$  using  $e^+e^- \rightarrow \text{hadrons}$  data, to the semileptonic  $\tau$  decays case (focusing on the dominant two-pion contribution). Our main results are collected in Table 4 and show that  $\tau$ -based results are compatible with the lattice evaluations in the intermediate



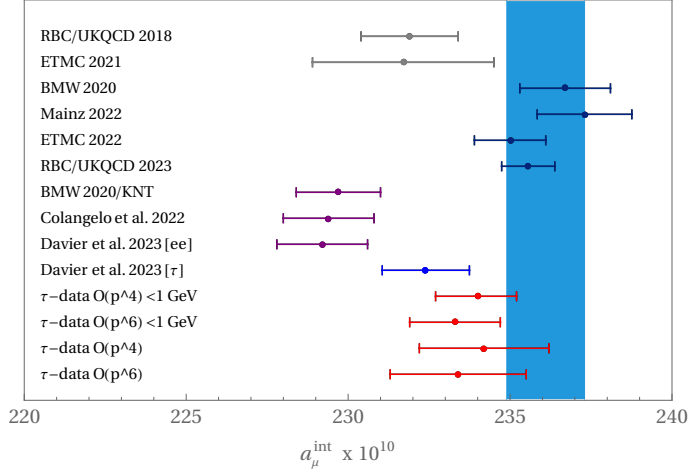


Figure 4: Comparison of the total intermediate window contribution to  $a_\mu^{\text{HVP, LO}}$ . The blue band corresponds to the weighted average of the lattice results excluding RBC/UKQCD 2018 [12] and ETMC 2021 [148].

window, being the  $e^+e^-$ -based values in tension with both of them. This difference is the main cause for the larger discrepancy of the latter with  $a_\mu^{\text{Exp}}$  and should be further scrutinized. Supplemented by the relevant IB corrections computed on the lattice [106], the results in this work could be used together with lattice QCD to obtain an alternative data-based determination from  $\tau$  decays (and lattice QCD) which can be helpful in solving the present puzzle.

## Acknowledgements

We have benefited from discussions with Rafel Escribano on this topic. We are indebted to Michel Davier, Gabriel López Castro, Bogdan Malaescu and Zhiqing Zhang for extremely useful discussions and detailed comparisons of our mutual results. It is always instructive and enlightening to learn something from Vincenzo Cirigliano. The work of P. M. has been supported by the European Union’s Horizon 2020 Research and Innovation Programme under grant 824093 (H2020-INFRAIA-2018-1), the Ministerio de Ciencia e Innovación under grant PID2020-112965GB-I00, and by the Secretaria d’Universitats i Recerca del Departament d’Empresa i Coneixement de la Generalitat de Catalunya under grant 2021 SGR 00649. IFAG is partially funded by the CERCA program of the Generalitat de Catalunya. J. A. M. is also supported by MICINN with funding from European Union NextGenerationEU (PRTR-C17.I1) and by Generalitat de Catalunya. P. R. thanks partial funding from Conacyt and Cátedras Marcos Moshinsky 2020 (Fundación Marcos Moshinsky).

## References

- [1] B. Abi et al. Measurement of the Positive Muon Anomalous Magnetic Moment to 0.46 ppm. *Phys. Rev. Lett.*, 126(14):141801, 2021.
- [2] G. W. Bennett et al. Final Report of the Muon E821 Anomalous Magnetic Moment Measurement at BNL. *Phys. Rev. D*, 73:072003, 2006.
- [3] Michel Davier, Andreas Hoecker, Bogdan Malaescu, and Zhiqing Zhang. Reevaluation of the hadronic vacuum polarisation contributions to the Standard Model predictions of the muon  $g - 2$  and  $\alpha(m_Z^2)$  using newest hadronic cross-section data. *Eur. Phys. J. C*, 77(12):827, 2017.
- [4] Alexander Keshavarzi, Daisuke Nomura, and Thomas Teubner. Muon  $g - 2$  and  $\alpha(M_Z^2)$ : a new data-based analysis. *Phys. Rev. D*, 97(11):114025, 2018.
- [5] Gilberto Colangelo, Martin Hoferichter, and Peter Stoffer. Two-pion contribution to hadronic vacuum polarization. *JHEP*, 02:006, 2019.

- [6] Martin Hoferichter, Bai-Long Hoid, and Bastian Kubis. Three-pion contribution to hadronic vacuum polarization. *JHEP*, 08:137, 2019.
- [7] M. Davier, A. Hoecker, B. Malaescu, and Z. Zhang. A new evaluation of the hadronic vacuum polarisation contributions to the muon anomalous magnetic moment and to  $\alpha(\mathbf{m}_Z^2)$ . *Eur. Phys. J. C*, 80(3):241, 2020. [Erratum: *Eur.Phys.J.C* 80, 410 (2020)].
- [8] Alexander Keshavarzi, Daisuke Nomura, and Thomas Teubner.  $g - 2$  of charged leptons,  $\alpha(M_Z^2)$ , and the hyperfine splitting of muonium. *Phys. Rev. D*, 101(1):014029, 2020.
- [9] Alexander Kurz, Tao Liu, Peter Marquard, and Matthias Steinhauser. Hadronic contribution to the muon anomalous magnetic moment to next-to-next-to-leading order. *Phys. Lett. B*, 734:144–147, 2014.
- [10] B. Chakraborty et al. Strong-Isospin-Breaking Correction to the Muon Anomalous Magnetic Moment from Lattice QCD at the Physical Point. *Phys. Rev. Lett.*, 120(15):152001, 2018.
- [11] Sz. Borsanyi et al. Hadronic vacuum polarization contribution to the anomalous magnetic moments of leptons from first principles. *Phys. Rev. Lett.*, 121(2):022002, 2018.
- [12] T. Blum, P. A. Boyle, V. Gülpers, T. Izubuchi, L. Jin, C. Jung, A. Jüttner, C. Lehner, A. Portelli, and J. T. Tsang. Calculation of the hadronic vacuum polarization contribution to the muon anomalous magnetic moment. *Phys. Rev. Lett.*, 121(2):022003, 2018.
- [13] D. Giusti, V. Lubicz, G. Martinelli, F. Sanfilippo, and S. Simula. Electromagnetic and strong isospin-breaking corrections to the muon  $g - 2$  from Lattice QCD+QED. *Phys. Rev. D*, 99(11):114502, 2019.
- [14] Eigo Shintani and Yoshinobu Kuramashi. Study of systematic uncertainties in hadronic vacuum polarization contribution to muon  $g - 2$  with 2+1 flavor lattice QCD. *Phys. Rev.*, D100(3):034517, 2019.
- [15] C. T. H. Davies et al. Hadronic-vacuum-polarization contribution to the muon’s anomalous magnetic moment from four-flavor lattice QCD. *Phys. Rev.*, D101(3):034512, 2020.
- [16] Antoine Gérardin, Marco Cè, Georg von Hippel, Ben Hörz, Harvey B. Meyer, Daniel Mohler, Konstantin Ottnad, Jonas Wilhelm, and Hartmut Wittig. The leading hadronic contribution to  $(g - 2)_\mu$  from lattice QCD with  $N_f = 2 + 1$  flavours of  $O(a)$  improved Wilson quarks. *Phys. Rev. D*, 100(1):014510, 2019.
- [17] Christopher Aubin, Thomas Blum, Cheng Tu, Maarten Golterman, Chulwoo Jung, and Santiago Peris. Light quark vacuum polarization at the physical point and contribution to the muon  $g - 2$ . *Phys. Rev.*, D101(1):014503, 2020.
- [18] D. Giusti and S. Simula. Lepton anomalous magnetic moments in Lattice QCD+QED. *PoS, LATTICE2019*:104, 2019.
- [19] Kirill Melnikov and Arkady Vainshtein. Hadronic light-by-light scattering contribution to the muon anomalous magnetic moment revisited. *Phys. Rev.*, D70:113006, 2004.
- [20] Pere Masjuan and Pablo Sánchez-Puertas. Pseudoscalar-pole contribution to the  $(g_\mu - 2)$ : a rational approach. *Phys. Rev.*, D95(5):054026, 2017.
- [21] Gilberto Colangelo, Martin Hoferichter, Massimiliano Procura, and Peter Stoffer. Dispersion relation for hadronic light-by-light scattering: two-pion contributions. *JHEP*, 04:161, 2017.
- [22] Martin Hoferichter, Bai-Long Hoid, Bastian Kubis, Stefan Leupold, and Sebastian P. Schneider. Dispersion relation for hadronic light-by-light scattering: pion pole. *JHEP*, 10:141, 2018.
- [23] Antoine Gérardin, Harvey B. Meyer, and Andreas Nyffeler. Lattice calculation of the pion transition form factor with  $N_f = 2 + 1$  Wilson quarks. *Phys. Rev.*, D100(3):034520, 2019.
- [24] Johan Bijnens, Nils Hermansson-Truedsson, and Antonio Rodríguez-Sánchez. Short-distance constraints for the HLbL contribution to the muon anomalous magnetic moment. *Phys. Lett.*, B798:134994, 2019.
- [25] Gilberto Colangelo, Franziska Hagelstein, Martin Hoferichter, Laetitia Laub, and Peter Stoffer. Longitudinal short-distance constraints for the hadronic light-by-light contribution to  $(g - 2)_\mu$  with large- $N_c$  Regge models. *JHEP*, 03:101, 2020.

- [26] Vladyslav Pauk and Marc Vanderhaeghen. Single meson contributions to the muon’s anomalous magnetic moment. *Eur. Phys. J.*, C74(8):3008, 2014.
- [27] Igor Danilkin and Marc Vanderhaeghen. Light-by-light scattering sum rules in light of new data. *Phys. Rev.*, D95(1):014019, 2017.
- [28] Friedrich Jegerlehner. The Anomalous Magnetic Moment of the Muon. *Springer Tracts Mod. Phys.*, 274:pp.1–693, 2017.
- [29] M. Knecht, S. Narison, A. Rabemananjara, and D. Rabetiarivony. Scalar meson contributions to  $a_\mu$  from hadronic light-by-light scattering. *Phys. Lett.*, B787:111–123, 2018.
- [30] Gernot Eichmann, Christian S. Fischer, and Richard Williams. Kaon-box contribution to the anomalous magnetic moment of the muon. *Phys. Rev. D*, 101(5):054015, 2020.
- [31] Pablo Roig and Pablo Sánchez-Puertas. Axial-vector exchange contribution to the hadronic light-by-light piece of the muon anomalous magnetic moment. *Phys. Rev.*, D101(7):074019, 2020.
- [32] Gilberto Colangelo, Martin Hoferichter, Andreas Nyffeler, Massimo Passera, and Peter Stoffer. Remarks on higher-order hadronic corrections to the muon  $g-2$ . *Phys. Lett. B*, 735:90–91, 2014.
- [33] Thomas Blum, Norman Christ, Masashi Hayakawa, Taku Izubuchi, Luchang Jin, Chulwoo Jung, and Christoph Lehner. The hadronic light-by-light scattering contribution to the muon anomalous magnetic moment from lattice QCD. *Phys. Rev. Lett.*, 124(13):132002, 2020.
- [34] Tatsumi Aoyama, Masashi Hayakawa, Toichiro Kinoshita, and Makiko Nio. Complete Tenth-Order QED Contribution to the Muon  $g-2$ . *Phys. Rev. Lett.*, 109:111808, 2012.
- [35] Tatsumi Aoyama, Toichiro Kinoshita, and Makiko Nio. Theory of the Anomalous Magnetic Moment of the Electron. *Atoms*, 7(1):28, 2019.
- [36] Andrzej Czarnecki, William J. Marciano, and Arkady Vainshtein. Refinements in electroweak contributions to the muon anomalous magnetic moment. *Phys. Rev. D*, 67:073006, 2003. [Erratum: *Phys.Rev.D* 73, 119901 (2006)].
- [37] C. Gnendiger, D. Stöckinger, and H. Stöckinger-Kim. The electroweak contributions to  $(g-2)_\mu$  after the Higgs boson mass measurement. *Phys. Rev. D*, 88:053005, 2013.
- [38] T. Aoyama et al. The anomalous magnetic moment of the muon in the Standard Model. *Phys. Rept.*, 887:1–166, 2020.
- [39] G. Colangelo et al. Prospects for precise predictions of  $a_\mu$  in the Standard Model. *arXiv: 2203.15810 [hep-ph]*, 3 2022.
- [40] Johan Bijnens, Nils Hermansson-Truedsson, Laetitia Laub, and Antonio Rodríguez-Sánchez. Short-distance HLbL contributions to the muon anomalous magnetic moment beyond perturbation theory. *JHEP*, 10:203, 2020.
- [41] En-Hung Chao, Antoine Gérardin, Jeremy R. Green, Renwick J. Hudspith, and Harvey B. Meyer. Hadronic light-by-light contribution to  $(g-2)_\mu$  from lattice QCD with SU(3) flavor symmetry. *Eur. Phys. J. C*, 80(9):869, 2020.
- [42] Gilberto Colangelo, Martin Hoferichter, and Peter Stoffer. Constraints on the two-pion contribution to hadronic vacuum polarization. *Phys. Lett. B*, 814:136073, 2021.
- [43] Bai-Long Hoid, Martin Hoferichter, and Bastian Kubis. Hadronic vacuum polarization and vector-meson resonance parameters from  $e^+e^- \rightarrow \pi^0\gamma$ . *Eur. Phys. J. C*, 80(10):988, 2020.
- [44] Pere Masjuan, Pablo Roig, and Pablo Sanchez-Puertas. The interplay of transverse degrees of freedom and axial-vector mesons with short-distance constraints in  $g-2$ . *J. Phys. G*, 49(1):015002, 2022.
- [45] Jan Lüdtkke and Massimiliano Procura. Effects of longitudinal short-distance constraints on the hadronic light-by-light contribution to the muon  $g-2$ . *Eur. Phys. J. C*, 80(12):1108, 2020.
- [46] Johan Bijnens, Nils Hermansson-Truedsson, Laetitia Laub, and Antonio Rodríguez-Sánchez. The two-loop perturbative correction to the  $(g-2)_\mu$  HLbL at short distances. *JHEP*, 04:240, 2021.

- [47] Luigi Cappiello, Oscar Catà, and Giancarlo D’Ambrosio. Scalar resonances in the hadronic light-by-light contribution to the muon  $(g-2)$ . *Phys. Rev. D*, 105(5):056020, 2022.
- [48] En-Hung Chao, Renwick J. Hudspith, Antoine Gérardin, Jeremy R. Green, Harvey B. Meyer, and Konstantin Ottnad. Hadronic light-by-light contribution to  $(g-2)_\mu$  from lattice QCD: a complete calculation. *Eur. Phys. J. C*, 81(7):651, 2021.
- [49] Gilberto Colangelo, Martin Hoferichter, Bastian Kubis, Malwin Niehus, and Jacobo Ruiz de Elvira. Chiral extrapolation of hadronic vacuum polarization. *Phys. Lett. B*, 825:136852, 2022.
- [50] Gilberto Colangelo, Franziska Hagelstein, Martin Hoferichter, Laetitia Laub, and Peter Stoffer. Short-distance constraints for the longitudinal component of the hadronic light-by-light amplitude: an update. *Eur. Phys. J. C*, 81(8):702, 2021.
- [51] Igor Danilkin, Martin Hoferichter, and Peter Stoffer. A dispersive estimate of scalar contributions to hadronic light-by-light scattering. *Phys. Lett. B*, 820:136502, 2021.
- [52] Martin Hoferichter and Thomas Teubner. Mixed Leptonic and Hadronic Corrections to the Anomalous Magnetic Moment of the Muon. *Phys. Rev. Lett.*, 128(11):112002, 2022.
- [53] Josef Leutgeb and Anton Rebhan. Hadronic light-by-light contribution to the muon  $g-2$  from holographic QCD with massive pions. *Phys. Rev. D*, 104(9):094017, 2021.
- [54] Ángel Miramontes, Adnan Bashir, Khépani Raya, and Pablo Roig. Pion and Kaon box contribution to  $a_\mu^{\text{HLbL}}$ . *Phys. Rev. D*, 105(7):074013, 2022.
- [55] Marvin Zanke, Martin Hoferichter, and Bastian Kubis. On the transition form factors of the axial-vector resonance  $f_1(1285)$  and its decay into  $e^+e^-$ . *JHEP*, 07:106, 2021.
- [56] Volodymyr Biloshytskyi, En-Hung Chao, Antoine Gérardin, Jeremy R. Green, Franziska Hagelstein, Harvey B. Meyer, Julian Parrino, and Vladimir Pascalutsa. Forward light-by-light scattering and electromagnetic correction to hadronic vacuum polarization. *JHEP*, 03:194, 2023.
- [57] Gilberto Colangelo, Martin Hoferichter, Bastian Kubis, and Peter Stoffer. Isospin-breaking effects in the two-pion contribution to hadronic vacuum polarization. *JHEP*, 10:032, 2022.
- [58] Johan Bijnens, Nils Hermansson-Truedsson, and Antonio Rodríguez-Sánchez. Constraints on the hadronic light-by-light in the Melnikov-Vainshtein regime. *JHEP*, 02:167, 2023.
- [59] Diogo Boito, Maarten Golterman, Kim Maltman, and Santiago Peris. Evaluation of the three-flavor quark-disconnected contribution to the muon anomalous magnetic moment from experimental data. *Phys. Rev. D*, 105(9):093003, 2022.
- [60] Diogo Boito, Maarten Golterman, Kim Maltman, and Santiago Peris. Data-based determination of the isospin-limit light-quark-connected contribution to the anomalous magnetic moment of the muon. *Phys. Rev. D*, 107(7):074001, 2023.
- [61] Dominik Stamen, Deepti Hariharan, Martin Hoferichter, Bastian Kubis, and Peter Stoffer. Kaon electromagnetic form factors in dispersion theory. *Eur. Phys. J. C*, 82(5):432, 2022.
- [62] T. Blum et al. Update of Euclidean windows of the hadronic vacuum polarization. *Phys. Rev. D*, 108(5):054507, 2023.
- [63] Jan Lüdtke, Massimiliano Procura, and Peter Stoffer. Dispersion relations for hadronic light-by-light scattering in triangle kinematics. *JHEP*, 04:125, 2023.
- [64] M. Davier, D. Díaz-Calderón, B. Malaescu, A. Pich, A. Rodríguez-Sánchez, and Z. Zhang. The Euclidean Adler function and its interplay with  $\Delta\alpha_{\text{QED}}^{\text{had}}$  and  $\alpha_s$ . *JHEP*, 04:067, 2023.
- [65] Shi-Jia Wang, Zhen Fang, and Ling-Yun Dai. Two body final states production in electron-positron annihilation and their contributions to  $(g-2)_\mu$ . *JHEP*, 07:037, 2023.
- [66] Sz. Borsanyi et al. Leading hadronic contribution to the muon magnetic moment from lattice QCD. *Nature*, 593(7857):51–55, 2021.
- [67] Marco Cè et al. Window observable for the hadronic vacuum polarization contribution to the muon  $g-2$  from lattice QCD. *Phys. Rev. D*, 106(11):114502, 2022.

- [68] C. Alexandrou et al. Lattice calculation of the short and intermediate time-distance hadronic vacuum polarization contributions to the muon magnetic moment using twisted-mass fermions. *Phys. Rev. D*, 107(7):074506, 2023.
- [69] G. Colangelo, A. X. El-Khadra, M. Hoferichter, A. Keshavarzi, C. Lehner, P. Stoffer, and T. Teubner. Data-driven evaluations of Euclidean windows to scrutinize hadronic vacuum polarization. *Phys. Lett. B*, 833:137313, 2022.
- [70] Genessa Benton, Diogo Boito, Maarten Golterman, Alex Keshavarzi, Kim Maltman, and Santiago Peris. Data-driven determination of the light-quark connected component of the intermediate-window contribution to the muon  $g - 2$ . *arXiv: 2306.16808 [hep-ph]*, 6 2023.
- [71] Christoph Lehner and Aaron S. Meyer. Consistency of hadronic vacuum polarization between lattice QCD and the R-ratio. *Phys. Rev. D*, 101:074515, 2020.
- [72] Gen Wang, Terrence Draper, Keh-Fei Liu, and Yi-Bo Yang. Muon  $g-2$  with overlap valence fermions. *Phys. Rev. D*, 107(3):034513, 2023.
- [73] Christopher Aubin, Thomas Blum, Maarten Golterman, and Santiago Peris. Muon anomalous magnetic moment with staggered fermions: Is the lattice spacing small enough? *Phys. Rev. D*, 106(5):054503, 2022.
- [74] Alexei Bazavov et al. Light-quark connected intermediate-window contributions to the muon  $g-2$  hadronic vacuum polarization from lattice QCD. *Phys. Rev. D*, 107(11):114514, 2023.
- [75] D. P. Aguillard et al. Measurement of the Positive Muon Anomalous Magnetic Moment to 0.20 ppm. 8 2023.
- [76] F. V. Ignatov et al. Measurement of the  $e^+e^- \rightarrow \pi^+\pi^-$  cross section from threshold to 1.2 GeV with the CMD-3 detector. *arXiv: 2302.08834 [hep-ex]*, 2 2023.
- [77] F. V. Ignatov et al. Measurement of the pion formfactor with CMD-3 detector and its implication to the hadronic contribution to muon ( $g-2$ ). *arXiv: 2302.08834 [hep-ex]*, 9 2023.
- [78] R. R. Akhmetshin et al. Reanalysis of hadronic cross-section measurements at CMD-2. *Phys. Lett. B*, 578:285–289, 2004.
- [79] V. M. Aul’chenko et al. Measurement of the pion form-factor in the range 1.04-GeV to 1.38-GeV with the CMD-2 detector. *JETP Lett.*, 82:743–747, 2005.
- [80] V. M. Aul’chenko et al. Measurement of the  $e^+e^- \rightarrow \pi^+\pi^-$  cross section with the CMD-2 detector in the 370 - 520-MeV c.m. energy range. *JETP Lett.*, 84:413–417, 2006.
- [81] R. R. Akhmetshin et al. High-statistics measurement of the pion form factor in the rho-meson energy range with the CMD-2 detector. *Phys. Lett. B*, 648:28–38, 2007.
- [82] M. N. Achasov et al. Update of the  $e^+e^- \rightarrow \pi^+\pi^-$  cross-section measured by SND detector in the energy region  $400\text{-MeV} < s^{*}(1/2) < 1000\text{-MeV}$ . *J. Exp. Theor. Phys.*, 103:380–384, 2006.
- [83] M. N. Achasov et al. Measurement of the  $e^+e^- \rightarrow \pi^+\pi^-$  process cross section with the SND detector at the VEPP-2000 collider in the energy region  $0.525 < \sqrt{s} < 0.883$  GeV. *JHEP*, 01:113, 2021.
- [84] F. Ambrosino et al. Measurement of  $\sigma(e^+e^- \rightarrow \pi^+\pi^-\gamma(\gamma))$  and the dipion contribution to the muon anomaly with the KLOE detector. *Phys. Lett. B*, 670:285–291, 2009.
- [85] F. Ambrosino et al. Measurement of  $\sigma(e^+e^- \rightarrow \pi^+\pi^-)$  from threshold to  $0.85\text{ GeV}^2$  using Initial State Radiation with the KLOE detector. *Phys. Lett. B*, 700:102–110, 2011.
- [86] D. Babusci et al. Precision measurement of  $\sigma(e^+e^- \rightarrow \pi^+\pi^-\gamma)/\sigma(e^+e^- \rightarrow \mu^+\mu^-\gamma)$  and determination of the  $\pi^+\pi^-$  contribution to the muon anomaly with the KLOE detector. *Phys. Lett. B*, 720:336–343, 2013.
- [87] A. Anastasi et al. Combination of KLOE  $\sigma(e^+e^- \rightarrow \pi^+\pi^-\gamma(\gamma))$  measurements and determination of  $a_\mu^{\pi^+\pi^-}$  in the energy range  $0.10 < s < 0.95\text{ GeV}^2$ . *JHEP*, 03:173, 2018.
- [88] J. P. Lees et al. Precise Measurement of the  $e^+e^- \rightarrow \pi^+\pi^-(\gamma)$  Cross Section with the Initial-State Radiation Method at BABAR. *Phys. Rev. D*, 86:032013, 2012.

- [89] M. Ablikim et al. Measurement of the  $e^+e^- \rightarrow \pi^+\pi^-$  cross section between 600 and 900 MeV using initial state radiation. *Phys. Lett. B*, 753:629–638, 2016. [Erratum: *Phys.Lett.B* 812, 135982 (2021)].
- [90] T. K. Pedlar et al. Precision measurements of the timelike electromagnetic form-factors of pion, kaon, and proton. *Phys. Rev. Lett.*, 95:261803, 2005.
- [91] S. Actis et al. Quest for precision in hadronic cross sections at low energy: Monte Carlo tools vs. experimental data. *Eur. Phys. J. C*, 66:585–686, 2010.
- [92] Francisco Campanario, Henryk Czyż, Janusz Gluza, Tomasz Jeliński, Germán Rodrigo, Szymon Tracz, and Dmitry Zhuridov. Standard model radiative corrections in the pion form factor measurements do not explain the  $a_\mu$  anomaly. *Phys. Rev. D*, 100(7):076004, 2019.
- [93] Fedor Ignatov and Roman N. Lee. Charge asymmetry in  $e^+e^- \rightarrow \pi^+\pi^-$  process. *Phys. Lett. B*, 833:137283, 2022.
- [94] Gilberto Colangelo, Martin Hoferichter, Joachim Monnard, and Jacobo Ruiz de Elvira. Radiative corrections to the forward-backward asymmetry in  $e^+e^- \rightarrow \pi^+\pi^-$ . *JHEP*, 08:295, 2022.
- [95] Ricard Alemany, Michel Davier, and Andreas Hocker. Improved determination of the hadronic contribution to the muon ( $g-2$ ) and to  $\alpha(M_Z)$  using new data from hadronic tau decays. *Eur. Phys. J. C*, 2:123–135, 1998.
- [96] V. Cirigliano, G. Ecker, and H. Neufeld. Isospin violation and the magnetic moment of the muon. *Phys. Lett. B*, 513:361–370, 2001.
- [97] V. Cirigliano, G. Ecker, and H. Neufeld. Radiative tau decay and the magnetic moment of the muon. *JHEP*, 08:002, 2002.
- [98] M. Davier, A. Hoecker, G. Lopez Castro, B. Malaescu, X. H. Mo, G. Toledo Sanchez, P. Wang, C. Z. Yuan, and Z. Zhang. The Discrepancy Between tau and  $e^+e^-$  Spectral Functions Revisited and the Consequences for the Muon Magnetic Anomaly. *Eur. Phys. J. C*, 66:127–136, 2010.
- [99] Michel Davier, Andreas Hoecker, Bogdan Malaescu, and Zhiqing Zhang. Reevaluation of the Hadronic Contributions to the Muon  $g-2$  and to  $\alpha(M_Z)$ . *Eur. Phys. J. C*, 71:1515, 2011. [Erratum: *Eur.Phys.J.C* 72, 1874 (2012)].
- [100] Michel Davier, Andreas Höcker, Bogdan Malaescu, Chang-Zheng Yuan, and Zhiqing Zhang. Update of the ALEPH non-strange spectral functions from hadronic  $\tau$  decays. *Eur. Phys. J. C*, 74(3):2803, 2014.
- [101] J. A. Miranda and P. Roig. New  $\tau$ -based evaluation of the hadronic contribution to the vacuum polarization piece of the muon anomalous magnetic moment. *Phys. Rev. D*, 102:114017, 2020.
- [102] J. A. Miranda and P. Roig. Effective-field theory analysis of the  $\tau^- \rightarrow \pi^-\pi^0\nu_\tau$  decays. *JHEP*, 11:038, 2018.
- [103] Vincenzo Cirigliano, Adam Falkowski, Martín González-Alonso, and Antonio Rodríguez-Sánchez. Hadronic  $\tau$  Decays as New Physics Probes in the LHC Era. *Phys. Rev. Lett.*, 122(22):221801, 2019.
- [104] Sergi González-Solís, Alejandro Miranda, Javier Rendón, and Pablo Roig. Exclusive hadronic tau decays as probes of non-SM interactions. *Phys. Lett. B*, 804:135371, 2020.
- [105] Vincenzo Cirigliano, David Díaz-Calderón, Adam Falkowski, Martín González-Alonso, and Antonio Rodríguez-Sánchez. Semileptonic tau decays beyond the Standard Model. *JHEP*, 04:152, 2022.
- [106] Mattia Bruno, Taku Izubuchi, Christoph Lehner, and Aaron Meyer. On isospin breaking in  $\tau$  decays for  $(g-2)_\mu$  from Lattice QCD. *PoS, LATTICE2018*:135, 2018.
- [107] Claude Bouchiat and Louis Michel. La résonance dans la diffusion méson  $\pi$ — méson  $\pi$  et le moment magnétique anormal du méson  $\mu$ . *J. Phys. Radium*, 22(2):121–121, 1961.
- [108] Loyal Durand. Pionic Contributions to the Magnetic Moment of the Muon. *Phys. Rev.*, 128:441–448, 1962.

- [109] Stanley J. Brodsky and Eduardo De Rafael. SUGGESTED BOSON - LEPTON PAIR COUPLINGS AND THE ANOMALOUS MAGNETIC MOMENT OF THE MUON. *Phys. Rev.*, 168:1620–1622, 1968.
- [110] M. Gourdin and E. De Rafael. Hadronic contributions to the muon g-factor. *Nucl. Phys. B*, 10:667–674, 1969.
- [111] S. Eidelman and F. Jegerlehner. Hadronic contributions to g-2 of the leptons and to the effective fine structure constant  $\alpha(M(z)^{**2})$ . *Z. Phys. C*, 67:585–602, 1995.
- [112] B. E. Lautrup and E. De Rafael. Calculation of the sixth-order contribution from the fourth-order vacuum polarization to the difference of the anomalous magnetic moments of muon and electron. *Phys. Rev.*, 174:1835–1842, 1968.
- [113] A. Sirlin. Radiative corrections to  $g(v)/g(\mu)$  in simple extensions of the  $su(2) \times u(1)$  gauge model. *Nucl. Phys. B*, 71:29–51, 1974.
- [114] A. Sirlin. Current Algebra Formulation of Radiative Corrections in Gauge Theories and the Universality of the Weak Interactions. *Rev. Mod. Phys.*, 50:573, 1978. [Erratum: *Rev. Mod. Phys.* 50, 905 (1978)].
- [115] A. Sirlin. Large  $m(W)$ ,  $m(Z)$  Behavior of the  $O(\alpha)$  Corrections to Semileptonic Processes Mediated by W. *Nucl. Phys. B*, 196:83–92, 1982.
- [116] W. J. Marciano and A. Sirlin. Radiative Corrections to beta Decay and the Possibility of a Fourth Generation. *Phys. Rev. Lett.*, 56:22, 1986.
- [117] W. J. Marciano and A. Sirlin. Electroweak Radiative Corrections to tau Decay. *Phys. Rev. Lett.*, 61:1815–1818, 1988.
- [118] William J. Marciano and A. Sirlin. Radiative corrections to  $\pi(\text{lepton } 2)$  decays. *Phys. Rev. Lett.*, 71:3629–3632, 1993.
- [119] Eric Braaten and Chong-Sheng Li. Electroweak radiative corrections to the semihadronic decay rate of the tau lepton. *Phys. Rev. D*, 42:3888–3891, 1990.
- [120] Jens Erler. Electroweak radiative corrections to semileptonic tau decays. *Rev. Mex. Fis.*, 50:200–202, 2004.
- [121] Julian S. Schwinger. *PARTICLES, SOURCES, AND FIELDS. VOL. 3.* 1989.
- [122] Manuel Drees and Ken-ichi Hikasa. Scalar top production in  $e^+e^-$  annihilation. *Phys. Lett. B*, 252:127–134, 1990.
- [123] D. Gómez Dumm and P. Roig. Dispersive representation of the pion vector form factor in  $\tau \rightarrow \pi\pi\nu_\tau$  decays. *Eur. Phys. J. C*, 73(8):2528, 2013.
- [124] Sergi Gonzàlez-Solís and Pablo Roig. A dispersive analysis of the pion vector form factor and  $\tau^- \rightarrow K^- K_S \nu_\tau$  decay. *Eur. Phys. J. C*, 79(5):436, 2019.
- [125] M. Davier, A. Hoecker, A. M. Lutz, B. Malaescu, and Z. Zhang. Tensions in  $e^+e^- \rightarrow \pi^+\pi^-(\gamma)$  measurements: the new landscape of data-driven hadronic vacuum polarization predictions for the muon  $g - 2$ . *arXiv: 2312.02053 [hep-ph]*, 12 2023.
- [126] Vincenzo Cirigliano, Wouter Dekens, Emanuele Mereghetti, and Oleksandr Tomalak. Effective field theory for radiative corrections to charged-current processes: Vector coupling. *Phys. Rev. D*, 108(5):053003, 2023.
- [127] G. Ecker, J. Gasser, A. Pich, and E. de Rafael. The Role of Resonances in Chiral Perturbation Theory. *Nucl. Phys. B*, 321:311–342, 1989.
- [128] G. Ecker, J. Gasser, H. Leutwyler, A. Pich, and E. de Rafael. Chiral Lagrangians for Massive Spin 1 Fields. *Phys. Lett. B*, 223:425–432, 1989.
- [129] V. Cirigliano, G. Ecker, M. Eidemuller, Roland Kaiser, A. Pich, and J. Portoles. Towards a consistent estimate of the chiral low-energy constants. *Nucl. Phys. B*, 753:139–177, 2006.
- [130] Karol Kampf and Jiri Novotny. Resonance saturation in the odd-intrinsic parity sector of low-energy QCD. *Phys. Rev. D*, 84:014036, 2011.

- [131] P. Roig, A. Guevara, and G. López Castro.  $VV'P$  form factors in resonance chiral theory and the  $\pi - \eta - \eta'$  light-by-light contribution to the muon  $g - 2$ . *Phys. Rev. D*, 89(7):073016, 2014.
- [132] A. Guevara, P. Roig, and J.J. Sanz-Cillero. Pseudoscalar pole light-by-light contributions to the muon  $(g - 2)$  in Resonance Chiral Theory. *JHEP*, 06:160, 2018.
- [133] Wen Qin, Ling-Yun Dai, and Jorge Portoles. Two and three pseudoscalar production in  $e^+e^-$  annihilation and their contributions to  $(g - 2)_\mu$ . *JHEP*, 03:092, 2021.
- [134] J. Gasser and H. Leutwyler. Chiral Perturbation Theory to One Loop. *Annals Phys.*, 158:142, 1984.
- [135] J. Gasser and H. Leutwyler. Chiral Perturbation Theory: Expansions in the Mass of the Strange Quark. *Nucl. Phys. B*, 250:465–516, 1985.
- [136] H. Leutwyler. On the foundations of chiral perturbation theory. *Annals Phys.*, 235:165–203, 1994.
- [137] F. Flores-Baez, A. Flores-Tlalpa, G. Lopez Castro, and G. Toledo Sanchez. Long-distance radiative corrections to the di-pion tau lepton decay. *Phys. Rev. D*, 74:071301, 2006.
- [138] A. Flores-Tlalpa, F. Flores-Baez, G. Lopez Castro, and G. Toledo Sanchez. Model-dependent radiative corrections to  $\tau^- \rightarrow \pi^- \pi^0 \nu$  revisited. *Nucl. Phys. B Proc. Suppl.*, 169:250–254, 2007.
- [139] J. J. Sakurai. Theory of strong interactions. *Annals Phys.*, 11:1–48, 1960.
- [140] Rafel Escribano, Alejandro Miranda, and Pablo Roig. Radiative corrections to the  $\tau^- \rightarrow (P_1 P_2)^- \nu_\tau$  ( $P_{1,2} = \pi, K$ ) decays. *arXiv: 2303.01362 [hep-ph]*, 3 2023.
- [141] Res Urech.  $\rho^0 - \omega$  mixing in chiral perturbation theory. *Phys. Lett. B*, 355:308–312, 1995.
- [142] Pablo Sanchez-Puertas, Enrique Ruiz Arriola, and Wojciech Broniowski. Baryonic content of the pion. *Phys. Lett. B*, 822:136680, 2021.
- [143] S. Schael et al. Branching ratios and spectral functions of tau decays: Final ALEPH measurements and physics implications. *Phys. Rept.*, 421:191–284, 2005.
- [144] M. Fujikawa et al. High-Statistics Study of the tau-  $\rightarrow$  pi- pi0 nu(tau) Decay. *Phys. Rev. D*, 78:072006, 2008.
- [145] S. Anderson et al. Hadronic structure in the decay tau-  $\rightarrow$  pi- pi0 neutrino(tau). *Phys. Rev. D*, 61:112002, 2000.
- [146] K. Ackerstaff et al. Measurement of the strong coupling constant  $\alpha(s)$  and the vector and axial vector spectral functions in hadronic tau decays. *Eur. Phys. J. C*, 7:571–593, 1999.
- [147] Michel Davier, Zoltan Fodor, Antoine Gerardin, Laurent Lellouch, Bogdan Malaescu, Finn M. Stokes, Kalman K. Szabo, Balint C. Toth, Lukas Varnhorst, and Zhiqing Zhang. Hadronic vacuum polarization: comparing lattice QCD and data-driven results in systematically improvable ways. *arXiv: 2308.04221 [hep-ph]*, 8 2023.
- [148] Davide Giusti and Silvano Simula. Window contributions to the muon hadronic vacuum polarization with twisted-mass fermions. *PoS, LATTICE2021*:189, 2022.